LA-UR-19-25966
Approved for public release; distribution is unlimited.

Title: Report on the effect of dopants on FLASH sintering of enhanced UO2

Author(s): Kardoulaki, Erofili

Intended for: Report

Issued: 2020-11-03 (rev.2)

APPENDIX E

NTRD DOCUMENT COVER SHEET [1]

Name/Title of Deliverable/Milestone/Revision No.	Report on the effect of dopants on FLASH sintering of enhanced UO2/ M3FT-19LA020201042
Work Package Title and Number	Advanced Synthesis and Fabrication of Ceramic Fuels - LANL/FT-19LA02020104
Work Package WBS Number	1.02.02.02.01
Responsible Work Package Manager	Erofili Kardoulaki (Name/Signature)
Date Submitted	06/27/19

Quality Rigor Level for Deliverable/Milestone[2]	☐ QRL-1 ☐ Nuclear Data	☐ QRL-2	☒ QRL-3	☐ QRL 4 Lab QA Program[3]

This deliverable was prepared in accordance with Los Alamos National Laboratory
(Participant/National Laboratory Name)

QA program which meets the requirements of
☒ DOE Order 414.1 ☐ NQA-1 ☐ Other

This Deliverable was subjected to:

☒ Technical Review

Technical Review (TR)

Review Documentation Provided

☐ Signed TR Report or,
☐ Signed TR Concurrence Sheet or,
☒ Signature of TR Reviewer(s) below

Name and Signature of Reviewers

Darrin Byler

☐ Peer Review

Peer Review (PR)

Review Documentation Provided

☐ Signed PR Report or,
☐ Signed PR Concurrence Sheet or,
☐ Signature of PR Reviewer(s) below

Name and Signature of Reviewers

NOTE 1: *Appendix E should be filled out and submitted with each deliverable. Or, if the PICS: NE system permits, completely enter all applicable information in the PICS: NE Deliverable Form. The requirement is to ensure that all applicable information is entered either in the PICS: NE system or by using the NTRD Document Cover Sheet.*

- *In some cases there may be a milestone where an item is being fabricated, maintenance is being performed on a facility, or a document is being issued through a formal document control process where it specifically calls out a formal review of the document. In these cases, documentation (e.g., inspection report, maintenance request, work planning package documentation or the documented review of the issued document through the document control process) of the completion of the activity, along with the Document Cover Sheet, is sufficient to demonstrate achieving the milestone.*

NOTE 2: *If QRL 1, 2, or 3 is not assigned, then the QRL 4 box must be checked, and the work is understood to be performed using laboratory QA requirements. This includes any deliverable developed in conformance with the respective National Laboratory / Participant, DOE or NNSA-approved QA Program.*

NOTE 3: *If the lab has an NQA-1 program and the work to be conducted requires an NQA-1 program, then the QRL-1 box must be checked in the work Package and on the Appendix E cover sheet and the work must be performed in accordance with the Lab's NQA-1 program. The QRL-4 box should not be checked.*

Report on the effect of dopants on FLASH sintering of enhanced UO_2

Nuclear Technology Research and Development

Prepared for
U.S. Department of Energy
FCRD Program
Erofili Kardoulaki
Los Alamos National Laboratory

06/28/19

M3FT-19LA020201042
LA-UR-19-25966

SUMMARY

Large grained UO_2 can be achieved through the addition of dopants such as, Cr, Al, Nb and Mg. The enhanced microstructure can enable slower fission gas release that reduces pressure build up in the fuel rods and better mechanical properties that can alter the pellet cracking behavior and, therefore, limit accident prone pellet cladding loading. UO_2 fuel is sintered through conventional sintering methods that require high temperatures and long sintering times. Field assisted sintering techniques like flash sintering use current and voltage to enable sintering of ceramics at low temperatures and short times. Flash sintering has been demonstrated for sintering UO_2 to high densities. In this work, this technique has been applied to Cr-doped UO_2 to assess the feasibility of the technique for grain enhancement. Doped UO_2 samples below and above the solubility limit of Cr into UO_2 have been assessed. The results show that grain enhancement was not possible in either case and this was attributed to the low temperatures and sintering times that make flash sintering attractive. For the Cr-doped sample below or near the solubility of Cr, it is postulated that the temperatures were not high enough to actually dissolve it into solution in the UO_2 lattice. For the Cr-doped sample above the solubility limit of Cr, secondary phases were identified via SEM and EDS, as expected. Follow up work should be carried out to assess if flash sintering can produce grain enlargement for UO_2 feedstocks with dopants already in solid solution such as UO_2 produced via sol-gel or modified direct denitration method.

CONTENTS

FIGURES

TABLES

ACRONYMS

AC	Alternating Current
AFC	Advanced Fuel Cycle
ATF	Accident Tolerant Fuel
DC	Direct Current
DIL	Dilatometer
DOE	Department of Energy
EBS	Ethylene Bis-Stearamide
FAST	Field Assisted Sintering Techniques
FS	Flash Sintering
FCRD	Fuel Cycle Research and Development
ICPMS	Inductively Coupled Plasma Mass Spectrometry
LANL	Los Alamos National Lab
LFA	Laser flash analyzer
LWR	Light Water Reactor
ORNL	Oak Ridge National Laboratory
O/M	Oxygen-to-Metal ratio
PPM	Parts per million
SEM	Scanning Electron Microscopy
SPS	Spark Plasma Sintering
TD	Theoretical Density
UHP	Ultra High Purity
wt%	Weight percent
XRD	X-Ray Diffraction

FCRD ADVANCED FUELS CAMPAIGN

1. INTRODUCTION

1.1 Additives in UO_2

Uranium dioxide is the primary fuel for nuclear reactors and has been in use for decades. Despite being a successful nuclear fuel with an established performance, the industry is always seeking for improvements. Such improvements relate to pellet-clad mechanical interactions with regard to pellet cracking behavior and fission gas (Xe and Kr) retention enhancement during reactor operation. Fission gas release causes an increase in the fuel rod pressure, which can in turn cause rod failure, as well as lower the thermal conductivity of the fuel-cladding gap. Large-grained UO_2 can reduce the release of fission gas and other fission products during operation [1] as well as change the microstructure-dependent nature of pellet cracking and associated contact loading on the cladding from the pellet. Additions of metal or rare earth oxides have been successfully used as additives that improve sinterability of UO_2 and enhance the grain size of the fuel. Typically, the grain size of doped UO_2 is an order of magnitude larger than that of undoped UO_2. Additions of Cr [2]–[6], Al [5]–[7], Nb [8]–[11], Mg [6], [12], [13], Ti [5], [7], [11], Y [7] and V [5], [7] have been studied as grain enlargers in UO_2. The dopants are usually added at hundred to thousand weight parts per million (ppm), often below or slightly above the solubility limit of the metal in the UO_2 lattice.

The interactions between dopant additions, grain size and fission gas release behavior are complex. The large grain size of the fuel is expected to reduce fission gas release [1], however, the doping does increase the diffusion coefficient of the fission gas, as seen in the work of Killeen on Cr-doped UO_2 [14]. This can result in cancelling out of the benefits of large grained, doped UO_2. To this date, the mechanisms via which the enhanced grain growth occurs in doped UO_2 are not fully understood. Liquid phase sintering has been proposed in the literature as the facilitating mechanism for enhanced grain growth [2], [15]. In Cr-doped UO_2 for example liquid phase sintering would be due to the existence of the CrO eutectic at 1950 K. Despite this, Bourgeois et al. [2] reported an increase in grain size as a function of Cr content for sintering temperatures below that of the CrO eutectic. In the same work, for temperatures below 1950 K, the largest grain size was observed at the solubility limit for Cr. For Cr content exceeding the solubility limit, the grain size was reduced. For temperatures above 1950 K, Cr additions above the solubility limit also resulted in increased grain size, due to liquid phase sintering. This suggests that Cr in solid solution within the UO_2 matrix is required to see the benefits of enlarged grains, or the sintering has to take place at high temperatures; above 1950 K for Cr-doped UO_2.

Conventional sintering is the typical mass scale fabrication route for nuclear fuel and has been used extensively to sinter doped UO_2. The conventional sintering temperatures can be as high as 1700 -1800 °C with sintering times of 4-5 hours at this temperature in order to obtain the necessary high density of >95% theoretical density (TD). There have been numerous efforts in an attempt to lower the sintering temperature to improve efficiency [16], [17]. However, any improvements made in sintering temperature still require long sintering times (hours) since the process is diffusion controlled. Field assisted sintering techniques (FAST) describe a group of novel sintering methods that use electric field and/or current to provide powder densification in very short time periods (minutes compared to hours) and at low temperatures compared to conventional sintering [18]. Spark plasma sintering (SPS) and flash sintering (FS) are FAST methods that have received a lot of attention in recent years due to their potential, significant economic impact. In FS, field and current are applied through the sample to sinter materials to high densities without adding pressure. Typically, a green density sample is placed in a furnace, in contact with two leads that are attached to a power supply [19], [20]. The flash event is characterized by a current runaway, in which the current exponentially increases until reaching a pre-defined current limit. The bulk of sintering can occur within seconds under the correct combination of field, current and temperature [6]. An example of the very high

sintering rates induced at relatively low temperatures via FS is shown in Figure 1 where UO_2 samples sintered conventionally and via FS are compared [21]. At 600 °C, rapid densification is observed in UO_2 with FS, conventional sintering results in no densification. The advantages of understanding and controlling the sintering mechanisms present in FS are, therefore, obvious.

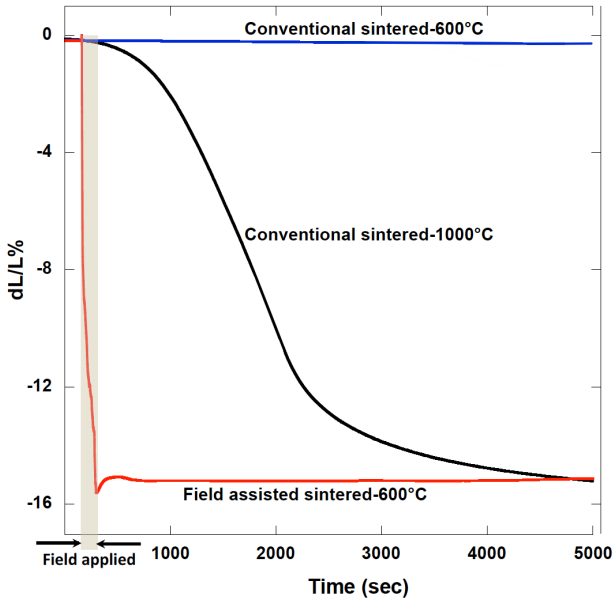

Figure 1: Densification profiles versus time for non-stoichiometric UO_2 samples sintered conventionally at 600 and 1000 °C and via FS at 600 °C [21]**.**

In this work the potential of using FS to fabricate Cr-doped UO_2 pellets has been examined. The goal here was to assess the resulting microstructures and comment on whether the addition of field and/or current has a beneficial or detrimental effect. Two dopant concentrations were examined in this work, one near (750 ppm Cr_2O_3) and one above (1500 ppm Cr_2O_3) the solubility limit of Cr into UO_2 [22]. The temperatures during FS are expected to be significantly lower than those needed to enable liquid phase sintering. However, it is noted that the exact temperature during FS has not been established.

2. EXPERIMENTAL PROCEDURE

2.1 Synthesis of doped UO_2 powder

The doped UO_2 powder is typically synthesized either via a dry route that uses mechanical milling of the UO_2 and the oxide powder [23], [24] or via a wet process where a chemical precursor is used to evenly distribute the dopant into the UO_2 [3], [7]. Recently, doped UO_2 has also been synthesized via an internal sol-gel approach at Oak Ridge National Laboratory (ORNL) [25]. In this work, a wet process was used as it is believed it produce a more uniform distribution of the oxide by fully coating the UO_2 particles. Chromium nitrate nonahydrate, $Cr(NO_3)_3 \bullet 9H_2O$, was used as the precursor as it is ethanol and water soluble and can be calcined to Cr_2O_3 at low temperatures, below 420 ˚C. The chromium nitrate precursor was dissolved in ethanol in the correct stoichiometry to produce the desired dopant amount, in this case 750 ppmw and 1500 ppmw. The precursor solutions were sonicated for 10 minutes to fully dissolve the precursor in ethanol and were then stored in Nalgene bottles and transferred to an inert atmosphere glovebox (<30 ppm O_2) for further processing. As-received depleted UO_2 from Areva (O/M=2.16) was milled in a high energy SPEX mill with a zirconia ball and vial for 15 minutes in 10g batches. The milled powder was

then passed through a 325-mesh sieve to ensure an agglomerate size of less than 44 μm. The sieved UO_2 was placed in a dedicated zirconia SPEX vial and hand blended with the precursor solution using a steel spatula for 1 minute, followed by SPEX milling with a zirconia ball for 5 minutes. This step was performed in batches of 10 g for the UO_2. Any remnants of the doped UO_2 solution in the SPEX jar were rinsed with an additional 2 ml of ethanol. The doped UO_2 solution was then placed on an alumina crucible, covered in aluminum foil, and heated to 500 ˚C for 1 hour under gettered ultra high purity (UHP) argon, flowing at 1 l/min. The calcined, doped powders were then crushed in a mortar and pestle to pulverize any larger particles, followed by sieving through a 325-mesh sieve. As a final step, the UO_2 was blended with 1 wt. % Ethylene Bis-Stearamide (EBS) to improve particle flow characteristics and handling of the green density pellets.

2.2 FS of UO_2

Pellets were pressed at 140 MPa with a dual action 4.49 mm punch and die set using a Carver 3851 uniaxial hydraulic hand press. A thin layer of Zinc Stearate was used to lubricate the punch and die surfaces that came in contact with the powder. The green density of the pressed pellets was approximately 60% theoretical density (TD). The ends of the pellets were coated in a thin layer of graphite paint to increase contact between the pellet and the graphite insulators that were placed between the platinum electrodes and the pellet. The graphite insulators served as an electrically conductive barrier used to minimize thermal losses during cool down. Previously, platinum paint, without any insulators between the electrodes and the pellet, was used but this set up resulted in significant cracking and often welding or partial melting of the pellet onto the platinum electrodes. The addition of the graphite insulators and graphite paint resulted in elimination of the aforementioned effects and in sintered, undoped UO_2 pellets with good mechanical integrity and minimal hourglassing.

The flash experiments were performed in a dilatometer (NETZSCH, DIL 402C) that was retrofitted with platinum contacts and leads connecting to a power supply (PELCO 20V, 20A). In this set up, described in more detail in [21], an electric field is applied through the sample, which is in contact with the platinum leads, while the sample is at a predefined isothermal temperature. This temperature was selected to increase the electrical conductivity of UO_2 such that the flow of current through the sample is instant, i.e. an incubation period is not manifested. That temperature was selected to be 600 ˚C where conventional sintering does not take place, therefore, eliminating any contributions other than from FS. The samples were first heated to 450 ˚C, at a rate of 10 ˚C/min, for half an hour to burn out the EBS binder. This was followed by heating to the maximum FS temperature, 600 ˚C in this case, also at a rate of 10 ˚C/min, and holding for 2 hours. The first 30 minutes of this isothermal hold were required to achieve isothermal heating of the DIL furnace. Once this was reached, FS was initiated.

A current control method was used in these FS experiments where a maximum pseudo alternating current (AC) was predefined along with a rate for increase and decrease of the current. The voltage was not defined in these experiments contrary to traditional FS as outlined in [21], [26] where direct current (DC) was used. A number of FS current control profiles were tested to select the appropriate current ramp up and ramp down rates as well as the maximum current density. All FS experiments, including all heating steps, were performed under gettered UHP argon flowing at 300 ml/min with an oxygen content of $< 10^{-14}$ ppm.

2.2.1 Density measurements and microstructural characterization

After sintering, the pellets were roughly ground using a 600 grit SiC grinding paper to remove any graphite paint from the ends of the pellet. The final density of the pellets was measured at room temperature via Archimedes immersion density. Following the density measurements, a portion of the sintered pellets were cut along their longitudinal axis to examine their microstructure along the length of the pellet. The sectioned pieces were mounted in epoxy and polished to be examined under a scanning electron microscope (SEM). A thin layer of graphite was painted on the polished sample surface to help with electrical conductivity.

The grain size of the examined samples was determined using the line intercept method. Approximately 20 intercepts were counted on each sample to enable good statistics of these measurements.

3. RESULTS

3.1 Synthesis of doped UO_2 powder

In Figure 2, SEM images of the starting Areva powder (a) used in to synthesize the 750 ppm Cr-doped UO_2 power (b) is shown. The resulting powder was examined to ensure that no abnormally large particles were present and to ensure that the powder was nominally spherical. In Bourgeois et al. [2] the Cr-doped powder was spray-dried and, therefore, resulted in spherical particles that aided flowability of the powder and resulted in well compacted pellets. The powder shown in Figure 2(b) was nominally spherical and therefore was expected to aid pellet compaction.

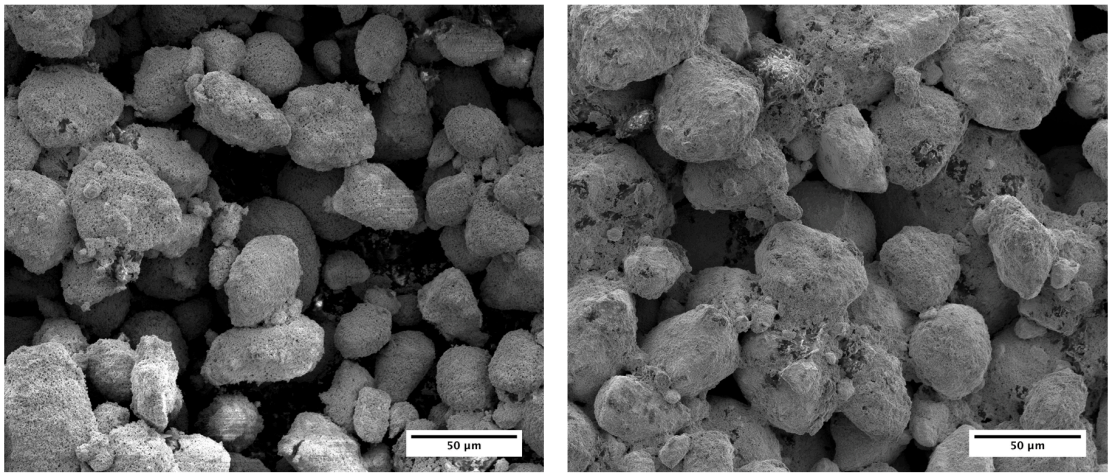

(a) (b)

Figure 2: SEM pictures of (a) Areva powder passed through a 325-mesh and (b) doped powder with 750 ppm Cr_2O_3 calcined at 500 ˚C.

3.2 Densification and initial microstructural characterization results

A number of FS conditions were tested to identify the optimal parameters for densification of the doped UO_2 pellets. The majority of this development phase was conducted with the 750ppm Cr-doped pellets. The parameters that were probed were the maximum current, the rate of increase of the current, the hold time and the sintering atmosphere. Figure 3, shows the resulting immersion densities achieved for samples tested under different current densities. All the samples shown in Figure 3 were tested with a current increase rate of 1A/min and a current decrease rate of 0.5A/min. All samples were held at the maximum current density for 2 minutes except for one sample, indicated in the figure, which was held for 10 minutes. It is obvious that immersion density increases almost linearly with increasing maximum current density. Current densities up to 600 mA/mm^2 where tested here as previous work [21] has shown detrimental effects to the samples if this value is exceeded. The effect of dwell time at maximum current density was also probed and it was found that a prolonged dwell, 10 minutes versus 2 minutes, results in a lower density. This is due to internal cracking in the sample resulting from a large power input in the sample for a prolonged time. Literature studies have also shown that a prolonged dwell time, longer than a few minutes, during FS at maximum current is not required [27]. Samples that were sintered under Ar-5%H_2 showed a reduction in resulting immersion density. This was expected as the reducing environment would limit the sintering kinetics. Finally, the effect of the current increase rate was examined and it was established that a rate

higher than 1 A/min resulted in lower immersion densities for all samples. This was further probed by comparing a sample that was sintered at nominally traditional FS conditions (sample 3, Table 1) versus a sample that was sintered at the current control FS conditions given for the samples of Figure 3 (sample 1, Table 1). Both these samples were sintered at a maximum current density of 600 mA/mm^2, however, the sample flashed with the current control method resulted in a higher density, namely 87.33 % TD versus 82.16 % TD for the nominally traditionally flashed sample. This is due to the instantaneous current increase rate during traditional FS of sample 3 which has resulted in thermal shock of the sample and, therefore, lower density due to significant internal cracking.

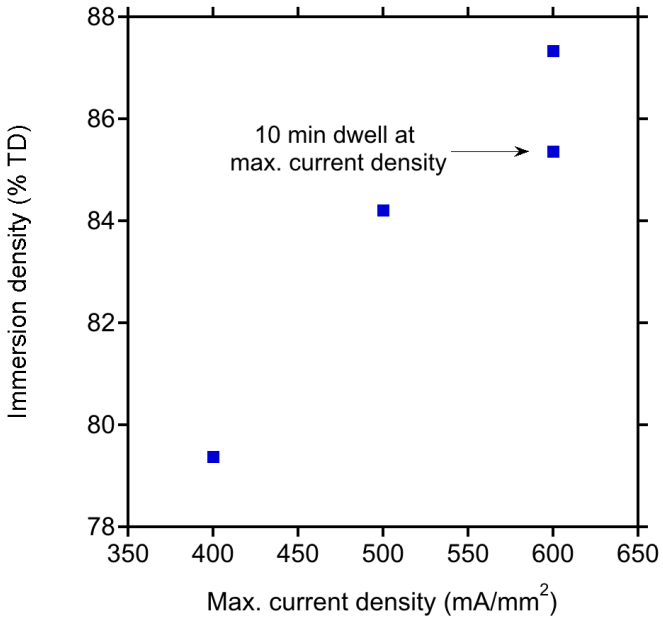

Figure 3: Immersion density versus maximum current density applied during FS experiments. FS was carried out at a furnace temperature of 600 ˚C. The current increase rate was set at 1 A/min while the current decrease was set at 0.5 A/min for all samples shown here. All samples except the one indicated in the figure were held at the maximum current density for 2 minutes. All samples shown here were sintered under getetred UHP Ar.

Table 1: List of sample IDs, Cr-doping content, FS conditions, and resulting immersion densities for 4 samples of interest that were further probed via optical microscopy.

Sample ID	Cr concentration (ppm)	Max. current density (mA/mm^2)	Current increase rate (A/min)	Current decrease rate (A/min)	Dwell time (min)	Immersion density (% TD)
1	750	600	1	0.5	2	87.33
2	750	600	1	0.5	10	85.36
3	750	600	instantaneous	0.5	2	82.16
4	1500	600	1	0.5	2	79.38

In Table 1 a list of the FS conditions, Cr-doping content, and resulting immersion densities is shown for 4 samples of interest that were selected to be examined under SEM. Sample 1 was tested under an FS profile that was deemed to procure the highest densities and resulted in an immersion density of 87.33% TD. Sample 2 was tested with a longer, 10 minute, dwell time, which resulted in a decrease in density, namely 85.36 % TD. Sample 3 was tested under conditions of nominally traditional FS, with the exception of a 0.5

A/min current decrease rate, and resulted also in a decrease in density, namely 82.16 % TD. The current decrease rate of 0.5 A/min was tested in an effort to minimize thermal shock of the sample, a phenomenon often encountered in traditional FS of UO_2 due to abrupt cooling. Sample 4 was tested with the same profile as that for Sample 1, however the increased Cr-doping content of 1500 ppm resulted in a significant decrease in density, namely 79.38 % TD. For reference, the FS current and voltage profiles of samples 1-3 are shown in Figure 4. Interestingly, identical FS conditions produce very different densification for a sample that is doped with 750 ppm Cr_2O_3, near the solubility limit of Cr into the UO_2 lattice, and a sample that is doped with 1500 ppm Cr_2O_3, above the solubility limit of Cr. According to Peres et al.[22] and Bourgeois et al. [2], additions of Cr above the solubility limit would result in the insoluble Cr_2O_3 to form secondary phase particles. These secondary phases could inhibit grain growth and densification by limiting grain boundary mobility. This would explain the density discrepancies between samples 1 and 4. It is noted that for all samples in this work, densities < 90% TD were obtained. This is likely caused due to the Cr additions in the UO_2 feedstock since densities >90% TD were previously obtained via FS [21].

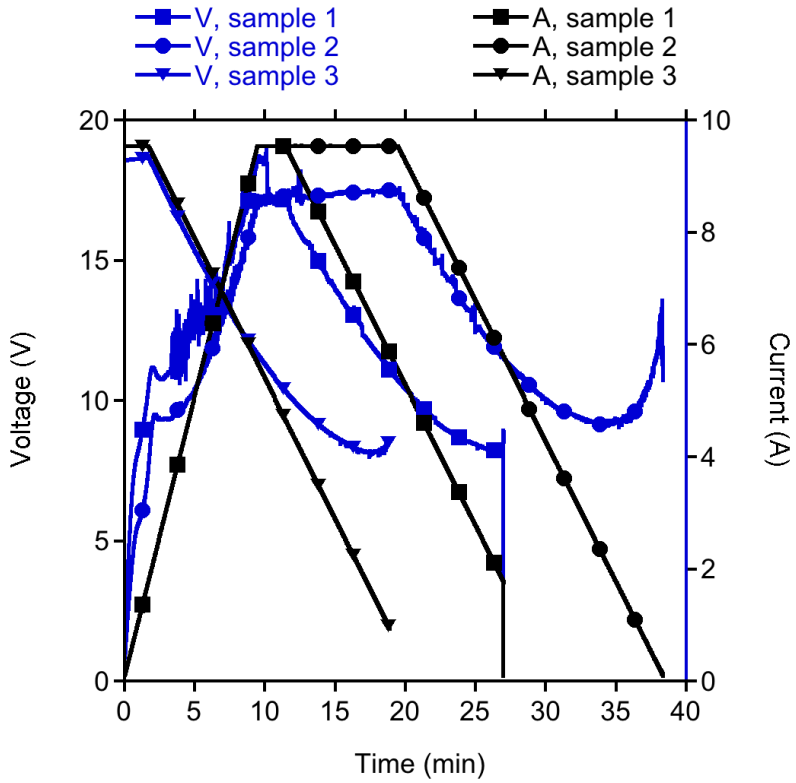

Figure 4: FS current and voltage profiles of samples 1-3 of Table 1. It is noted that sample 4, not shown here, has the same FS profile as sample 1.

Low magnification SEM images of samples 1-4 taken from cross-sections of their longitudinal axis, are shown in Figure 5. As expected, based on the immersion densities of Table 1, sample 1 (Figure 5(a)) features the microstructure with the least amount of internal cracking. Nonetheless, small scale cracking and significant porosity are still observed. In Figure 5(b), the microstructure of sample 2 is shown and, as expected based on the prolonged dwell time of 10 minutes, internal cracking is identified. However, the cracking is mostly located in the center of the pellet, while the outer regions feature high density areas. The sample that was sintered under nominally traditional FS conditions (Figure 5(c)) features significant internal cracking throughout the length of the pellet, with cracking extending from the inner to the outer areas of the sample. The microstructure of sample 3 is significantly worse than those of samples 1 and 2 indicating that the current increase rate, effectively the heating rate of the sample, is a significant parameter to control. It follows that a slow current increase rate, likely even slower than that applied for sample 1, would be

beneficial to achieve a well-controlled microstructure. Nonetheless, this proves that the use of the current control method in FS is a significant advantage over the traditional method where the current increases instantaneously to the pre-defined maximum current density. Finally, the increased Cr content of sample 4 (Figure 5(d)) seems to be negatively impacting the microstructure, thus, resulting in extensive cracking along the length of the pellet.

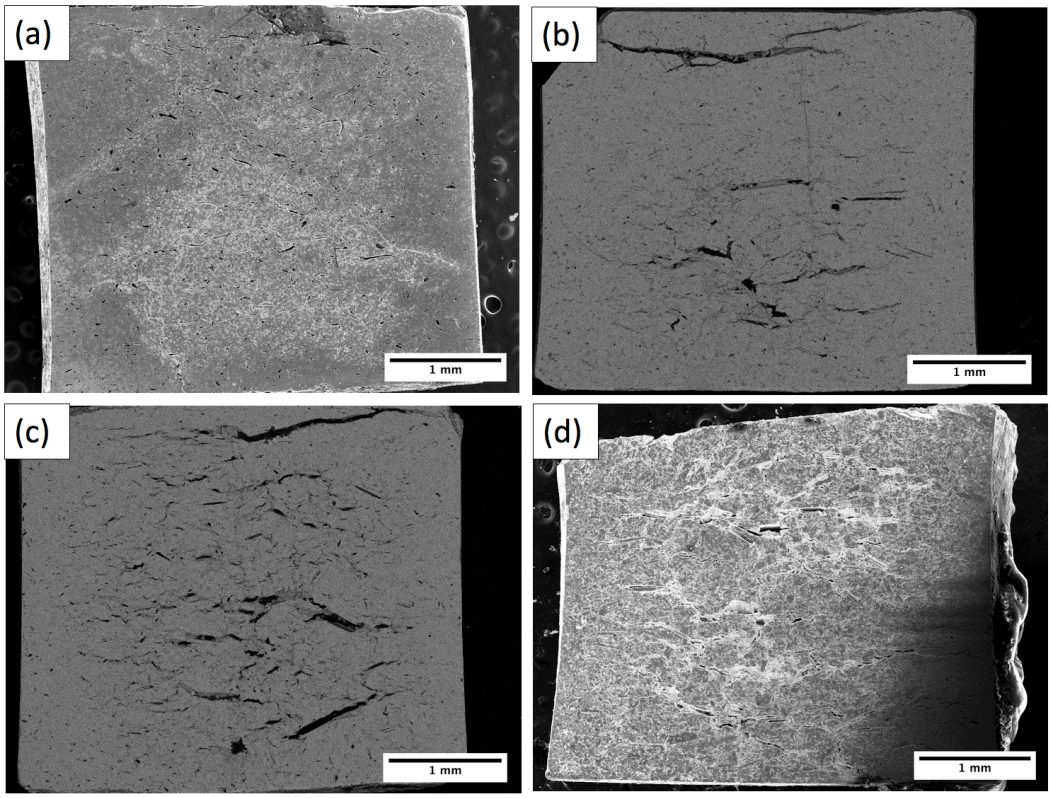

Figure 5: Low magnification SEM images obtained across the longitudinal cross section of (a) sample 1, (b) sample 2, (c) sample 3, and (d) sample 4. Samples 1-3 are doped with 750 ppm Cr_2O_3 while sample 4 is doped with 1500 ppm Cr_2O_3.

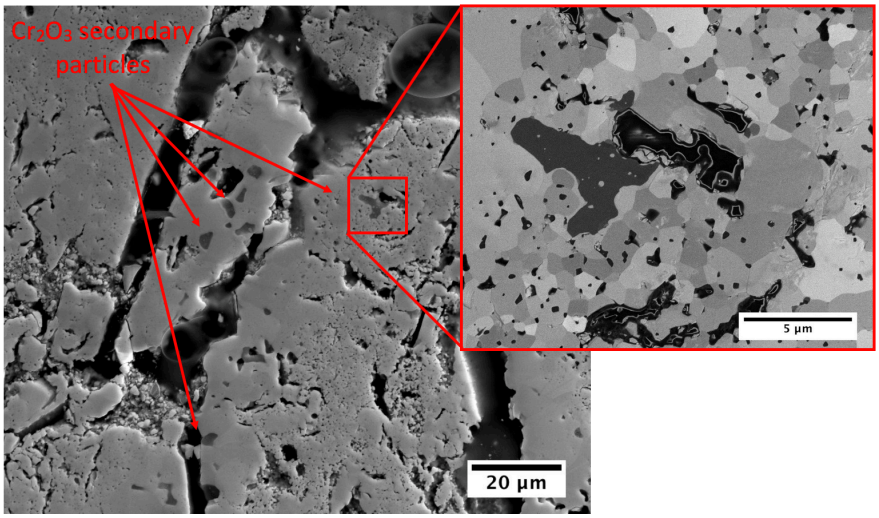

Figure 6: High magnification, backscatter, SEM images of sample 4, 1500 ppm Cr-doped UO_2, showing the presence of Cr_2O_3 secondary phases.

High magnification, backscatter SEM images of sample 4 are shown in Figure 6, confirming the presence of undissolved Cr_2O_3 secondary particles. The determination that these particles are Cr_2O_3 was performed via both backscatter microscopy and via energy dispersive spectroscopy (EDS) analysis, shown in Figure 7 and Table 2. The darker color of these phases indicates that they have low Z number and the EDS confirms the presence of Cr and O in these regions. It is noted that secondary phases were only identified for sample 4. Samples 1-3 did not show any indication that Cr_2O_3 formed secondary particles.

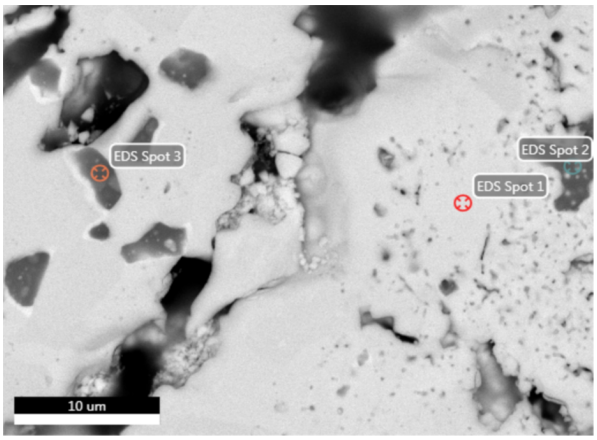

Figure 7: SEM image of sample 4 used for EDS spot analysis

Table 2: Results of EDS spot analysis for sample corresponding to the regions shown in Figure 7.

Atomic % (%)	O	U	Cr
EDS Spot 1	82	18	
EDS Spot 2	12.5	3	84.5
EDS Spot 3		2.9	97.1

Despite the fact that no evidence of secondary phases was found for samples doped with 750 ppm Cr, minimal enhancement in grain growth was seen in these samples. In particular, the average grain size of sample 1 was measured at 6.75 μm, while for sample 4 at 5.95 μm. The grain size distributions for both examined samples were non-uniform and grains of up to 25 μm as well as grains as small as 2 μm were identified in sample 1. Similarly, for sample 4 grains of up to 17 μm as well as grains as small as 1 μm were observed. SEM pictures of representative microstructures for sample 1 and 4 are shown in Figure 8(a) and 8(b), respectively. The key parameters affecting grain growth are temperature and partial pressure of oxygen. In this work, atmospheres of $<10^{-14}$ ppm O_2 were selected for the FS of samples 1-4 and the furnace temperature was kept constant at 600 ˚C. However, the actual sample temperature during FS is not known. During FS the thermocouple recording the temperature of the sample, located ~ 2 mm away from the sample, recorded a maximum of 800 ˚C. According to previous work [26] , the temperature during FS likely does not exceed 1000 ˚C. Therefore, as mentioned earlier, grain size enhancement due to liquid phase sintering was not expected. Instead, Cr going into solution into the UO_2 lattice was expected to be the mechanism by which grain enlargement was achieved. In the case of sample 4, the additions of Cr oxide above the solubility limit were predicted to result in no enhancing effect on the grain growth of the sample. However, sample 1 for which the Cr oxide content was under the solubility limit was expected to produce enlarged grains in line with the findings of Bourgeois [2]. Surprisingly, this was not the case and virtually no grain enhanced was observed either. Temperature could have played a crucial role here as the ~ 700 ppm solubility limit for Cr into UO_2 was established at a temperature of 1700 ˚C. During FS, it is unlikely that

the temperature will increase to 1700 ˚C and, therefore, it is possible that Cr_2O_3 did not dissolve into the lattice explaining the minimal grain enhancement. The fact that no secondary phases were identified in sample 1 could be due to volatilization of Cr_2O_3 in-situ. Inductive coupled plasma mass spectrometry (ICPMS) of the initial feedstock as well as of samples after FS should be conducted to investigate whether the Cr content changes during processing. Finally, the short timescales associated with FS would also inhibit grain growth as compared to conventional sintering. For reference, a comparison of the resulting microstructures fabricated via FS (a) and via conventional sintering (b) is shown in Figure 9 for 750 ppm Cr-doped UO_2 samples. From Figure 9 it is evident that conventional sintering produces significantly more uniform microstructures with larger grains. However, it is noted that a large grain size distribution was also observed in conventional sintering as well as extensive porosity.

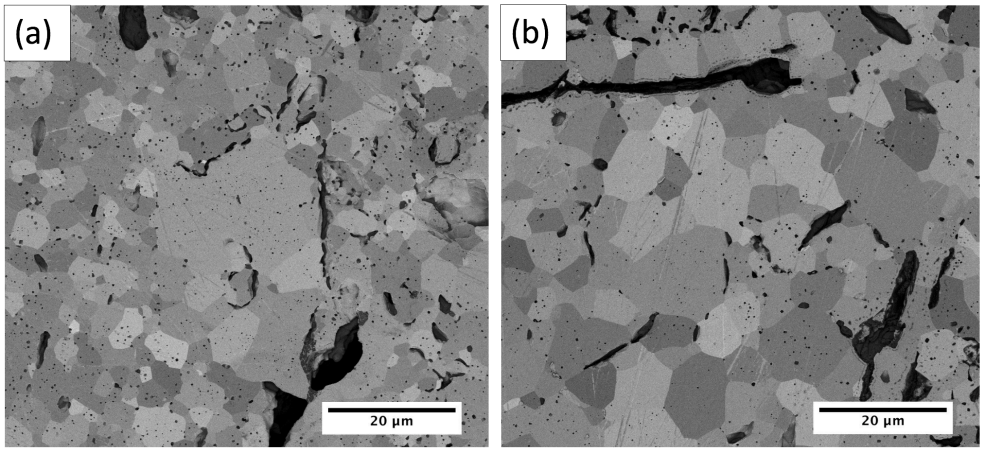

Figure 8: SEM images of (a) sample 1, 750 ppm Cr-doped UO_2 and (b) sample 4, 1500 ppm Cr-doped UO_2.

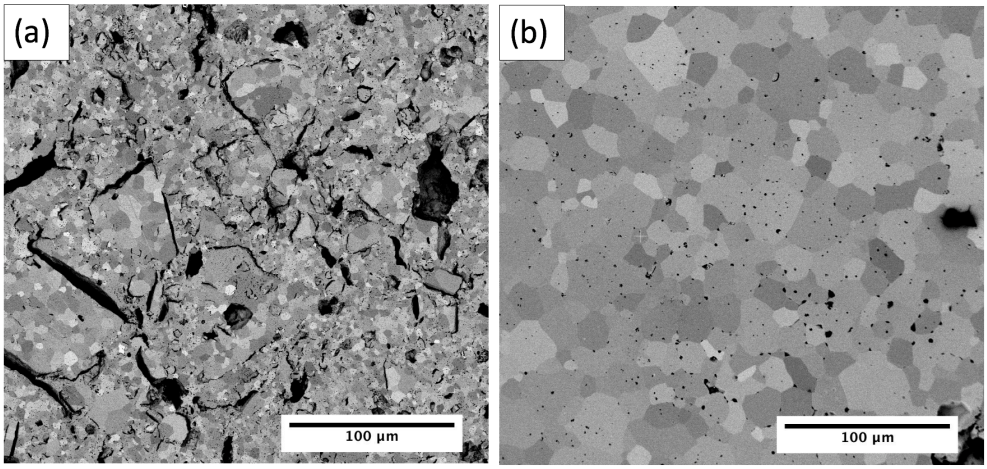

Figure 9: SEM images of (a) sample 1, sintered via FS and (b) a 750 ppm Cr-doped UO_2 sample sintered conventionally at 1600 ˚C for 4 hours.

4. CONCLUSIONS AND PATH FORWARD

FS for Cr-doped UO_2 has been assessed to identify whether this technique can be used to produce large grains. The results of this work indicate that FS is not a suitable technique for grain enlargement of doped UO_2. This finding is linked to the low temperatures exhibited during FS and the short timescales that are utilized; minutes versus hours for conventional sintering. In particular, the low temperatures during FS

likely inhibited Cr_2O_3 from going into solution into the UO_2 lattice and, therefore, impeded grain growth for the 750 ppm Cr-doped UO_2 sample. Additionally, liquid phase sintering could not have taken place during these FS conditions and, therefore, the samples with high Cr content, 1500 ppm, did not show any grain growth either. Instead, they formed second phase particles that impacted densification and grain growth, as expected. Evidence of Cr_2O_3 secondary particles was identified both via backscatter SEM and EDS analysis.

FS was not deemed suitable for grain enlargement, under the conditions tested in this study, due to the low temperatures and short timescales utilized in this fabrication technique. Interestingly, these are also the reasons for which this technique is of interest for UO_2 as well as other advanced fuel forms since it can provide significant cost improvements. Moreover, further evidence of relatively low sintering temperatures during FS indicate that the field and current do play a significant role in the densification of materials. The mechanism by which field and current enable rapid densification in UO_2 remains to be explained.

The proposed path forward to fully assess whether FS could be used as a way to sinter large grained, doped UO_2 would be to source feedstocks with dopants already in solution, like the sol-gel UO_2 feedstocks and the UO_2 feedstocks via a modified direct denitration (MDD) process [28], currently produced at ORNL. Especially for the case of feedstocks produced via MDD, the dopant additions would be integrated into the UO_2 lattice on the atomic scale. Therefore, using these feedstocks would clarify the effects of dopant content and whether going into solution provides a real benefit in grain enhancement or not. If the sol-gel and MDD feedstocks produce similar results as the ones shown in this work, then it would mean that the timescales in FS are too short to allow meaningful grain growth.

REFERENCES

[1] J. A. Turnbull, “The effect of grain size on the swelling and gas release properties of UO_2 during irradiation,” *J. Nucl. Mater.*, vol. 50, pp. 62–68, 1974.
[2] L. Bourgeois, P. Dehaudt, C. Lemaignan, and A. Hammou, “Factors governing microstructure development of Cr_2O_3-doped UO_2 during sintering,” *J. Nucl. Mater.*, vol. 297, pp. 313–326, 2001.
[3] D. Byler, “Grain growth kinetics of doped UO_2 for model development,” 2019.
[4] T. Cardinaels *et al.*, “Chromia doped UO_2 fuel: Investigation of the lattice parameter,” *J. Nucl. Mater.*, vol. 424, pp. 252–260, 2012.
[5] M. T. Aybers *et al.*, “Grain growth in corundum oxides-doped uranium dioxide and effects of grain growth to the mechanical properties of uranium dioxide such as elasticity determined by ultrasonic methods,” *Key Eng. Mater.*, vol. 264–268, pp. 985–988, 2004.
[6] S. Kashibe and K. Une, “Effect of additives (Cr_2O_3 , Al_2O_3 , SiO_2 , MgO) on diffusional release of 133Xe from UO2 fuels,” *J. Nucl. Mater.*, pp. 234–242, 1998.
[7] R. M. Leckie and E. P. Luther, “Evolutionary enhancements to UO_2 pellets,” 2013.
[8] J. C. Killeen, “The effect of niobium oxide additions on the electrical conductivity of UO_2,” *J. Nucl. Mater.*, vol. 88, pp. 185–192, 1980.
[9] H. Assmann, W. Dorr, G. Gradel, G. MAier, and M. Peehs, “Doping UO_2 with niobia - Beneficial or not?,” *J. Nucl. Mater.*, vol. 98, pp. 216–220, 1981.
[10] G. Marsh, G. A. Wood, and C. P. Perkins, “Niobia-doped UO_2 fuel manufacturing Experience at BNFL,” *Tech. Comm. Meet. Adv. fuel pellet Technol. Improv. Perform. high Burn.*, vol. 1996, 1996.
[11] K. Une, I. Tanabe, and M. Oguma, “Effects of additives and the oxygen potential on the fission gas diffusion in UO_2 fuel,” *J. Nucl. Mater.*, vol. 150, pp. 93–99, 1987.
[12] P. T. Sawbridge, C. Baker, R. M. Cornell, K. W. Jones, D. Reed, and J. B. Ainscough, “The irradiation performance of magnesia-doped UO_2 fuel,” *J. Nucl. Mater.*, vol. 95, pp. 119–128, 1980.
[13] T. Fujino, S. Nakama, N. Sato, and K. Yamada, “Solubility of magnesium in uranium dioxide,” *J.*

Nucl. Mater., vol. 246, pp. 150–157, 1997.
[14] J. C. Killeen, "Fission gas release and swelling in UO_2 doped with Cr_2O_3," *J. Nucl. Mater.*, vol. 88, pp. 177–184, 1980.
[15] V. Peres *et al.*, "High temperature chromium volatilization from Cr_2O_3 powder and Cr_2O_3 -doped UO2 pellets in reducing atmospheres," *J. Nucl. Mater.*, vol. 423, pp. 93–101, 2012.
[16] X. Yang, J. Gao, Y. Wang, and X. Chang, "Low-temperature sintering process for UO_2 pellets in partially-oxidative atmosphere," *Trans. Nonferrous Met. Soc. China (English Ed.*, vol. 18, no. 1, pp. 171–177, 2008.
[17] N. Fuhrman, L. D. Hower, and R. B. Holden, "Low-Temperature Sintering of Uranium Dioxide," *J. Am. Ceram. Soc.*, vol. 46, no. 3, 1963.
[18] R. Raj, M. Cologna, and J. S. C. Francis, "Influence of externally imposed and internally generated electrical fields on grain growth, diffusional creep, sintering and related phenomena in ceramics," *J. Am. Ceram. Soc.*, vol. 94, no. 7, pp. 1941–1965, 2011.
[19] J. A. Downs and V. M. Sglavo, "Electric field assisted sintering of cubic zirconia at 390 ˚C," *J. Am. Ceram. Soc.*, vol. 96, no. 5, pp. 1342–1344, 2013.
[20] S. Grasso *et al.*, "Modeling of the temperature distribution of flash sintered zirconia," *J. Ceram. Soc. Japan*, vol. 119, no. 1386, pp. 144–146, 2011.
[21] J. A. Valdez, D. D. Byler, E. Kardoulaki, J. S. C. Francis, and K. J. Mcclellan, "Flash sintering of stoichiometric and hyper-stoichiometric urania," *J. Nucl. Mater.*, vol. 505, pp. 85–93, 2018.
[22] V. Peres, L. Bourgeois, and P. Dehaudt, "Grain growth and Ostwald ripening in chromia-doped uranium dioxide," *J. Phys. IV*, vol. 3, pp. 1477–1480, 1993.
[23] B. J. Dooies, "Enhancement of uranium dioxide thermal and mechanical properties by oxide dopants," 2008.
[24] J. Arborelius *et al.*, "Advanced Doped UO_2 Pellets in LWR Applications," *J. Nucl. Sci. Technol.*, vol. 43, no. 9, pp. 967–976, 2006.
[25] S. C. Finkeldei *et al.*, "Synthesis and characterization of UO_2 feedstocks containing controlled dopents," 2019.
[26] D. J. Sprouster *et al.*, "In situ X-ray characterization of uranium dioxide during flash sintering," *Materialia*, vol. 2, no. June, pp. 176–182, 2018.
[27] J. S. C. Francis and R. Raj, "Influence of the field and the current limit on flash sintering at isothermal furnace temperatures," *J. Am. Ceram. Soc.*, vol. 96, no. 9, pp. 2754–2758, 2013.
[28] R. Vedder, "Summary of FY12 oxide powder synthesis and process development effort," 2012.